ingegneria sismica
International Journal of Earthquake Engineering
Anno XLIII - Num. 2 - 2026

Research on Lightweight and Robust High-Resolution DOA Estimation for Millimeter-Wave Radar Based on lightweight multiple signal classification algorithm

Tianlong Yang[1,*], *Jinqiu Dong*[1] *and Zixiang Long*[2]

[1] School of Electronic and Information Engineering, Liaoning Technical University, Huludao 125105, Liaoning, China
[2] Faculty of Electrical and Control Engineering, Liaoning Technical University, Huludao 125105, Liaoning, China

SUMMARY: *The traditional Direction-of-Arrival (DOA) estimation methods include Fast Fourier Transform beamforming, Multiple Signal Classification (MUSIC), Compressed Sensing or Orthogonal Matching Pursuit (CS/OMP), etc., which have varying performance characteristics in terms of computation speed, spectral resolution and sparse recovery. They have not yet achieved the optimal state of a good compromise between estimation accuracy, computation cost and real-time performance in complicated mmWave radar scenarios. DOA estimation at this stage in radar-based target identification, tracking, and recognitions; Its accuracy directly impacts the subsequent processing steps of these functions. To solve the above problem, this paper presents an improved lightweight multiple Signal Classification algorithm (L-MUSIC). In light of the trade-offs often suffered by methods such as FFT, MUSIC and CS/OOMP, L-MUSIC introduces the MUSIC subspace-processing chain into its basic realization structure and alleviates computational intensity problems caused by covariances, eigenvalues, full-angles spectra calculations via recursive covariance estimation; adaptive dimensional reduction techniques (such as SVD), rapid update method for subspaces, two-stage angle search strategies. Candidate-angle filtering and local spectral evaluation further reduce the load on a full-angular domain spectrum search. To suppress the sub-space degradation due to multiple paths propagation and coherent interference, and to reduce the performance drop caused by model discrepancy in the array-based system, we propose a novel strategy that adds diagonal-loading pre-processing and forward-backward spatial-smoothing post-processing techniques. Experiments show that L-MUSIC has a larger concentration of its primary lobe, an increased low-frequency null with respect to untargeted angles, stronger sidelobes and spurs peak suppression performance. The estimating error of the proposed method is lower than that for other comparative schemes at all tested SNR levels; Compared with these schemes' identifying success rate increases further under high SNR scenarios. At Close-angle Dual-Target, Low-Snapshot, Coherent-Source Conditions, L-MUSIC remains very discriminative; also shows high Resolution Performance and good Stability at this time. Computational cost-wise, compared with traditional MUSIC and CS/OMP, L-MUSIC's average execution time is relatively short, yet it still has excellent performance in arrays' position deviations. These results indicate that L-MUSIC provides a lightweight high-resolution solution to the common trade-off among estimation performance, computational efficiency, and robustness in FFT, MUSIC, and CS/OMP methods, and therefore ofA feasible way to estimate the distance continuously based on Continuous-Doppler-Attenuation.fers an effective approach for real-*

*15942371946@163.com
https://doi.org/10.65102/is2026808
Published: 30 April, 2026

time DOA estimation in complex scenarios.

KEYWORDS: *Adaptive dimension reduction; Direction-of-arrival estimation; Millimeter-wave radar; Recursive covariance updating; Two-stage angular search*

1 Introduction

In recent years, spectral analysis techniques have been the focus of many studies on modern signal-processing methods for detecting targets; they are necessary to assess how well a particular system performs. With the development and application of radar, communication and Acoustic technologies constantly advancing in tandem; therefore, a greater number must be built that can accurately perform spectrographic analysis in actual environments. Moreover, nonstationary Signals, multiple target interferes, and changing Noise Environment Have made the spectral Estimation technology more Adaptable and Stronger Robustness Requirements Have Arisen. Given that many scholars are engaged in investigations on Frequency Domain Analysis based upon the FFT method due to its efficiency and practicality for calculation.

The Fast Fourier Transform (FFT) can detect the spectrum of a signal effectively; henceforth, it is often called Radar Communication Sonar system Signal analysis' basic method in recent years. Kurtoglu Emre and Mohammad and Mahbubur Rahman [3] used an array of methods to process the echo from frequency-modulated continuous wave radar to estimate target range, velocity, orientation etc. Zhu Zhaojing, Chen Yanqiao, Lu Xiaoying: Proposed using a frequency domain method based on FFT to study nodes' pressures in water supply networks [4, 5]; Thus being able to judge pipeline operation condition and locate leak points by observing spectra signals. Renjie Huang and Hongyng Huang [6] used the FFT for real-time audio spectrum analysis, added an automatic gain control (AGC), and achieved dynamic volume regulation. Donciu Codrin, Temneanu Marinel Costel and Serea Elena in [7] proposed a direct oversampling technique using non-integer repetition factors inside the FFT kernel. Their approach can achieve similar spectral-Analysis results as the zero-Padding Oversampled scheme at significantly lower computational costs. Oussama Khouili, Mohamed Hanine et al. [8] presented the FFT-ShuffleNet approach that achieves high accuracy while being ultra-lightweight; therefore, it also reduces both latency and memory requirements simultaneously. The original FFT algorithm still has some defects in multi-object target signal processing at a low SNR and the environment with required spectral accuracy, etc. Mainly reflected in a widening of the main lobe and an elevation of the side-lobe; making it hard to distinguish between adjacent frequencies and thus decreasing frequency-estimation accuracy. Therefore, the practicability of use for high precision is still limited.

To avoid the limit of resolution in using FFT-based beamforming, MUSIC, which has better high-resolution characteristics based on subspace decomposition, can be used. Through eigenvalue decomposition of the Signal Covariance Matrix to separate the signal subspace from the Noise Subspace, thereby achieving much greater Spectral Resolution than traditional methods based on Fast Fourier Transform (FFT). Music has achieved relatively good results for application in array signal processing, bearing estimation and so on. Zhu Ping et al [9] proposed an improved MUSIC method that combines both directions of spatial smoothing to improve the accuracy of separating direct waves from reflected ones; It is also more stable in practice. Liu DongJia, Tao XiongJun and others [10] combined the application of Kalman filter with multiple signal classifiers to improve the Direction Of Arrival (DOA) performance in ultra high frequency Sensing Array. Li Xinting et al [11] have proposed an improved MUSIC algorithm based on the S transform that can no longer estimate the number of signals in advance but still

performs well under such conditions. Duo Li, Lei Chen, and other scholars [12] have integrated MUSIC principles into the reflectometry Matrix Method to propose a music-based reflectionometry Matrix Approach. It reduces image cluttering to improve the quality of the image. Mahgoun Hichem, Azmedroubbouzad [13] have suggested a novel approach combining Music inversion and statistical modelling of scatterers. Using a set of three volume scatterers to enhance the reconstruction precision of MUSIC in synthetic aperture radar tomography. Riku Takemoto, Jaesang Cha and others [14] have introduced a new Virtual-Antenna MUSIC-based DOA estimation method to enhance the accuracy of position identification more effectively. Yan Pan, Li Zhang et al [15] have proposed a simple one-bit MUSIC method for DOA estimation and achieved results similar to those of MUSIC-based methods with full simulation data. MUSIC has excellent performance, but owing to excessive computation every time, it is highly sensitive to changes in the array structure and significantly affected by fluctuations in Signal-to-Noise Ratio (SNR), making full application unfeasible under practical conditions. The problem of real-time handling resources scarcity situations, or the inability to complete processing requirements online.

Recently, Compressed Sensing or Orthogonal Matching Pursuit (CS/OMP) have offered some new ways to realize efficient Sparse- Signal reconstruction. Away from the Nyquist limit, CS/Omple method can accurately recover the signal and parameter under noisy conditions as it has been improved significantly by existing technologies. Zhou Xinran et al [16] introduced an adjustable target-image acquisition approach for visual Light-imaging Fuses using CS/OMPTheory; This technique can recover high-quality images from less-data- acquired signals. Zhong Shengyi and Qiao Ming proposed introducing an IFCW-SAR azimuth discontinuous-data reconstruction method based on CS/OMP to reduce the reliance of existing algorithms on a priori knowledge of scene sparsity in Reference [17]. Liu Yuanda, Zhang Huaying et al. [18]: proposed a method for detecting harmonics and interharmonics by combining the Nuttall-window-CS/OMPS technology with interpolation techniques to solve problems such as measurement error, data communication difficulty and storage problem. Zihan Lin and Shuhai Jia et al [19] presented a super-resolution phase-reconstruction technique using CS/OMP combined with deep learning in digital holographic microscopy; It has features of low redundant data storage, high-speed reconstruction speed and high-precision image restoration. Le Qin, Yukang Xu, et al. [20] have proposed the combined method of PC-BCSNet that integrates the pattern coupling sparse Bayesian learning framework based on classical statistical theory with data-driven deep-learning methods to enhance application flexibility and robustness in practice. Tianzhifu, Tao Hu et al [21] put forward an Frequency-Analysis Joint Optimisation Network for ICS that improves Attention on low-frequency and high-frequency components of Images. Although the CS/OMP algorithm needs to perform a complicated optimisation process. High computational load during iterative reconstruction, slow convergence speed; Also have a relatively high degree of parameter sensitivity. In terms of real-time response requirements and embedded devices, the computational demand for CS/OMPS will be higher still.

Overall, FFT, MUSIC and CS/Omp can be divided into the following categories: each has its own merits in terms of speed of computation, level of spectral separation and characteristics of sparse reconstruction [22-30]; However, it still lacks some perfection. Several existing approaches have improved the accuracy of DOA estimation through various aspects, such as Subspace-Fitting, Sparse-Covariance-Reconstruction, Robust-Beamforming and Low-Complexity Implementation [31-40]. They offer necessary assistance for increasing accuracy, decreasing computational resources required and improving generalisation capabilities. Most of these existing approaches optimise individual links in the entire process link, and there is no unified light-weight framework capable of simultaneously guaranteeing high-resolution, low-computation, and strong performance. FFT is computationally lightweight but of low resolution.

Music provides a high resolution but is computationally expensive. CS/OMP can recover signals in the presence of weak sampling, but it is computationally expensive. Thus, traditional techniques are unable to meet the demands for high accuracy and speed in real-time low-power, or variable conditions of signals simultaneously.

To solve the existing problems of coordination difficulty for FFT, MUSIC and CS/Omp in resolution accuracy, computational load and application adaptability; This paper presents a new lightweight low-Rank-FFT (L-FMUSIC) DoA estimator that is easy to implement. Given that MUSIC provides an excellent sub-space estimation background and rich resolution capabilities, this study will use it as the primary reference to construct the entire process for realisation; at each stage (covariance update, Subspace extraction, Spectral search, robustness improvement) within the unified scheme. Specifically, recursive covariance update, adaptive Dimension Reduction, rapid Subspace Update, and a Two-Stage Angular Search are adopted to lower the computing load of Covariance Processing, eigendecomposition, and complete Angle Spectral Evaluation; In addition, diagonal Loading and Forward-Backward Spatial Smoothing were added to enhance the robustness in Low-SNR, Coherent Source, Array Mis-match situations. An eight-dimensional experimental study is carried out to compare FFT, traditional MUSIC, CS/OMP, L-MUSIC in eight dimensions: spectral shape and side-lobe suppression, performance under different SNR conditions; Computational complexity, resolution, robustness, low-SNR performance, and resolution performance when there are common sources. To determine if this method has achieved an overall balanced performance of high resolution, low computation cost and strong generalisation ability through these assessments.

2 L-MUSIC Mechanism and Problem Modelling

To improve efficiency in DoA (Direction of Arrival) estimation for millimetre-wave radar Systems Based on L-MUSIC Algorithm's System Model. Using a uniform linear Array(ULA) consisting of M elements to collect signals arriving in various Directions and estimating the target direction-of-arrival (DOA). Multipath fading effects and coherency issues at multiple transmit antennas are all included; hence, these factors affect the covariance matrix as a whole through explicit calculation during this process.

2.1 Array Signal Model

Let the ULA have M components. Assuming that the observation vector at the n-th element in an array operates under a narrowband far-field condition, it may be written as.

$$x(n) = A(\theta)s(n) + w(n), n = 1,2, \dots, N, \tag{1}$$

where, $x(n)$denotes the array observation vector; $s(n)$ is the complex envelope of K signal sources; $w(n)$ denotes additive white noise. In addition, $A(\theta) = [a(\theta_1), \dots, a(\theta_K)]$ represents the array steering matrix, while $\theta = [\theta_1, \dots, \theta_K]$ denotes the set of incident angles to be estimated.

In the ULA case, given that the array element spacing is d and the carrier wavelength is λ; then The directional vector in Direction will be expressed by formula.θ

$$a(\theta) = \left[1, \quad e^{-j\frac{2\pi d}{\lambda}\sin\theta}, \quad \dots, \quad e^{-j\frac{2\pi d}{\lambda}(M-1)\sin\theta}\right]^T \tag{2}$$

Under a millimetre-wave Radar system for this study, d is usually λ / 2.

Under ideal conditions, the output covariance matrix of an array is as follows.

$$R_{xx} = E\{x(n)x^H(n)\} \tag{3}$$

During practice, the sample covariance matrix is approximately equal to taking a smaller number of observations N.

$$\widehat{R}_{xx} = \frac{1}{N}\sum_{n=1}^{N} x(n)x^H(n), \tag{4}$$

where $(\cdot)^H$ denotes the conjugate transpose. When the frame rate is sufficiently high and the noise follows a white-noise model, $\widehat{R}_{xx}$ provides a reasonable approximation to R_{xx}.

Performing an eigenvector decomposition of the corresponding covariance matrix.

$$\widehat{R}_{xx} = U\Lambda U^H, \tag{5}$$

Here, $\Lambda = \mathrm{diag}(\lambda_1, \dots, \lambda_M)$ and the eigenvalues satisft $\lambda_1 \geq \cdots \geq \lambda_M$. The matrix $U = [u_1, \dots, u_M]$ is the corresponding eigen-vector matrix. Given that under the white-noise condition, the largest K eigenvalues belong to the signal subspace and the rest of the MK eigenvectors constitute the noise subspaces.−

$$U = [U_s U_n], \tag{6}$$

where U_s represents the basis of the signal subspace, whereas U_n represents the basis of the noise subspace.

Above, the above-signal Model, covariance Representation and eigen decomposition relationship serve as an overall Modelling basis for Subspace Separation, Spectrum Estimation and Algorithm Improvement in following parts. In particular, the Construction of covariance matrix, the extraction of eigensubspaces and the angular response form of steering vector correspond directly to the later improvement of L-MUSIC in covariance update, lightweight subspace processing and spectral search strategy, which are thus regarded as the theory origin of both methodological Design and experimental verification presented here. The sub-space based Signal Model and covariance formulations presented herein are in line with the classic theory basis of MUSIC, Subspace Decomposition and Spatial Smoothing Methods [22-30]. The same can provide a solid theoretical foundation for the following Design of L-MUSIC.

2.2 Problem Modelling

In view of this, in order to achieve accurate DOA estimation based on the above signals model, it needs to be transformed into finding a suitable covariance matrix that can accurately separate the source signal sub-space from the noise sub-space and locate its corresponding spectral peaks. Therefore, the problem that needs to be solved by this research is not only how to implement an ordinary subspace estimator, but also how to maintain its excellent resolution performance under reduced computational load conditions in actual observation situations while enhancing its robustness.

Studies related to this show that the main deficiencies of traditional Subspace Methods are: high computation demands for covariance processing and eigendecomposition; a reduction due to coherency among multiple signals and imperfect noise conditions; low robustness against model deviations [29, 30], etc. Although sparse recovery and covariance adjustment algorithms have improved the estimation accuracy under certain circumstances [31-34]; however, introducing extra optimisation costs makes them less practical for application in time-constrained systems.

From this, three needs will arise naturally. Firstly, to ensure that the algorithm can

distinguish between closely spaced targets reliably; Secondly, to preserve the resolution characteristics of MUSIC-based methods as much as possible during lightweight design; Secondly, due to the high computational complexity of conventional MUSIC algorithms in practice; even when using full-scale calculations for large datasets or extensive coverage during searches, there is still too much cost. Thirdly, at a lower Signal-Noise Ratio (SNR), due to poor quality of the subspaces' separation, the estimation accuracy and robustness will decrease accordingly.

Traditional MUSIC selects the signal subspace and noise subspace by decomposing the covariance matrix, and then evaluates the full-angle pseudo-spectrum to obtain the DOA estimation results. The reach of the recognition accuracy for this model is somewhat limited; there are still some shortcomings upon application. The first bottleneck is the covariance estimate problem; during batch processing, it must be summed up across all time points for multiple times under conditions of variable data volume. The second bottleneck problem of exhaustive eigen decomposition is that it requires high computation power to extract the noise subspaces from huge covariance matrices. The third restriction is spectrum matching; it must scan through a broad range at high density to cover all possibilities fully.

Based on the above analysis, this paper reconstitute the processing chain of conventional MUSIC to establish an integrated L-MUSIC system. According to the goal of maintaining close-range clarity; reducing computation load; And increase robustness to low signal-to-noise ratios (SNRs); Correlated sources as well as array misalignment. Organise this algorithm as a collection of functions for both realisations and objectives. The first group is composed of light-weight computation units, which include recursive covariance update, adaptive dimensional reduction, quick sub-space construction, dual-stage angular search, etc. To further reduce the costs associated with covariance calculation, eigenvalue decomposition and complete angle spectral matching. The second group is the robustness-boosting module, which includes diagonal loading and forward-backward Spatial Smoothing. To address the adverse impacts of covariance degradation, source coherency issues, and array model mismatches on the performance of DOA estimation.

The above problem construction does not only provide the theory foundation for the Design of L-MUSIC But also determine how to organise experimental verification. Assess the proposed method comprehensively by evaluating it across these eight criteria: spectrum Shape and Side-lobes Suppression, Performance Under Different SNR Conditions, Computational Complexity, Resolution, Stability, Robustness, Low-Snapshot Performance, And Resolutions in Coherent Source Scenarios. The eight evaluation items form a series of evidence related to resolutions, computational costs and stability needs; And it determines if L-MUSIC has shown better overall trade-off performance compared with other approaches like conventional MUSIC or CS/OMP methods.

3 L-MUSIC Algorithmic Enhancements

3.1 The Conventional MUSIC Algorithm

Conventional MUSIC estimation of DOA takes advantage of orthogonality in the signals' subspaces relative to that of noises.

In ideal Narrow Band Far-Field Conditions, if the array covariance matrix can be accurately obtained and met under white-noise assumptions; then its Steering Vector for an actual arrival angle should be orthogonal to this noise subspace.

$$a^{H}(\theta_k)U_n = 0, k = 1, \ldots, K \tag{7}$$

Based on this, identify the genuine direction of sources through a pseudo-spectrum obtained by projecting onto the noise subspace.

Let the noise subspace be represented by U_n. The MUSIC pseudo-spectrum is written as

$$P_{MUSIC}(\theta) = \frac{1}{a^H(\theta)U_n U_n^H a(\theta)}, \tag{8}$$

where $a(\theta)$ denotes the array steering vector corresponding to angle θ. When the scanning angle coincides with a true incident direction, the projection of the steering vector onto the noise subspace becomes minimal, and the pseudo-spectrum exhibits a prominent peak at that location. Conventional MUSIC therefore estimates the target DOAs by evaluating the pseudo-spectrum over a predefined angular grid and identifying the peak locations. When K signal sources are present, the first K dominant peaks are typically selected as the final estimates.

The pseudo-spectrum $P_{MUSIC}(\theta)$ is evaluated over the angular grid θ, and the peak location is taken as the DOA estimation result

$$\{\hat{\theta}_1, \ldots, \hat{\theta}_K\} = \arg\max_{\theta} P_{MUSIC}(\theta) \tag{9}$$

Traditional MUSIC has good spectral resolution under ideal circumstances and is thus considered the most typical sub-space-based DOA estimation algorithm. Its actual performance is highly dependent on factors such as the quality of covariance estimation, accuracy of eigendecomposition and completeness verification of a full-angle pseudo-spectrum. When there are fewer than expected snapshots, when SNR is low due to coherent noise, or if the array model deviates from reality under certain circumstances; in this case, the resolution performance, stability and computing efficiency of traditional MUSIC may all decline to varying degrees. Due to these limitations, a unified lightweight framework will be proposed in the following section for improving resolution-accuracy-effort balance under existing MUSIC principles.

3.2 The L-MUSIC algorithm

Due to their difficulties in simultaneously achieving high-resolution performance, low-computational requirements, and robustness in various environments for observing multiple targets, the L-MUSIC algorithm is proposed as a solution in this paper. FFT has a low computational cost and high resolution. Music has very high resolution; However, the process of covariance filtering, eigen-decomposition and full angle spectrum search is time-consuming. Sparse reconstructions are possible using CS/OMP, but the cost in terms of optimisation is typically higher. Therefore, none of these typical ways can achieve a reasonable balance among the requirements for accurate model estimation, fast computing speed and general applicability under complicated environments. Given that MUSIC has been established with a good Subspace Estimation base-stone and high-resolution capability, for comparison reasons, this paper will use it as its processing system foundation to unify the reconstruction process of covariance update, Sub-space Processing, spectral searching, and Robustification improvement.

Some existing researches on low-complexity direction-of-arrival (DOA) estimation, diagonal loading, spatial filtering and coherent-source reduction have laid essential theoretical basis for the current study [35-40]. Most of these studies enhance DOA estimation from various angles by controlling complexity, stabilising subspaces, reducing sources' correlation under coherency problems to some extent, but they often lack comprehensive consideration for an entire stage or part of a process during system design. Compared to this, the proposed L-MUSIC introduces covariance update, subspace processing, spectral searching capabilities, as well as

increased robustness for an all-inclusive optimisation strategy of the traditional MUSIC method. Preserving as much as possible the high resolution property of subspace-based spectral estimation in the design of L-MUSIC for reducing computational load while enhancing robustness against complex environments such as low signal-to-noise ratio (SNR), incomplete data, coherent sources and array misalignment.

Regarding its algorithmic Structure, L - MUSIC includes two kinds of function blocks. The first group includes the following light-weight computation modules: Recursive covariance update; Adaptive Dimension Reduction; Fast Subspace Update; Two-Stage Angular Search. The following modules will be introduced to lighten the computational load for covariance estimation, eigendecomposition, and full-angle spectrum calculation. The second Group consists of the following types: Diagonal Loading; forward-backward Spatial Smoothing. Modules listed above aim to enhance the ability of sub-space separation under low SNR, inadequate sampling, correlated sources, and mismatch in arrays. The coordinated work of these two kinds can go beyond the path optimisation plan of ordinary MUSIC to build a comprehensive lightweight, high-resolution system suitable for practical use. As shown in Figure 1, the overall Structure of this frame- work and implementations for each modules' development are described hereinafter to clarify their functions within the full-processing-chain process.

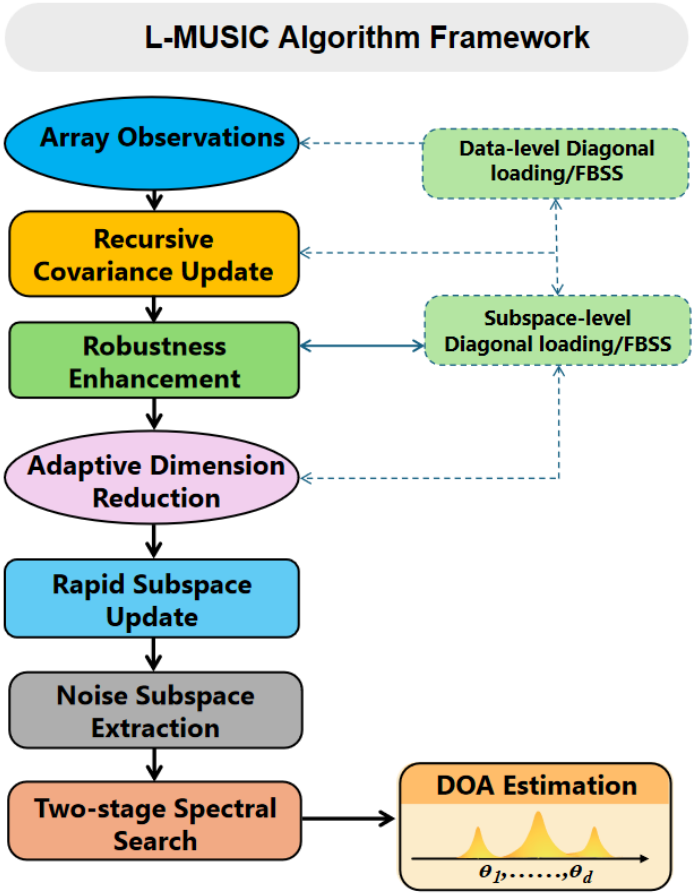

Figure 1: L-MUSIC algorithm framework.

Figure 1 shows the structure of the L-MUSIC algorithm. This diagram shows the entire process of applying L-MUSIC for array observation data and obtaining D.O.A.. Firstly, collect all the array data; Secondly, recursively calculate the covariances by updating them iteratively until it is done. To avoid redundant calculations, reduce the amount of data processed; At this

time, only keep necessary elements to ensure the accuracy of subsequent calculation processes. Based on this, the Robustness enhancement module introduces diagonal loading and forward-backward Spatial Smoothing (FBSS) at a complementary level of two parts: data-level pre-processing and Subspace Level Refinement, which can suppress Coherent Signal Degradation in Low-Snapshot Arrays due to poor arrays or covariances are not fully estimated. Then the algorithm performs adaptive dimension reduction and quick sub-space update to alleviate the problem of computing eigenvectors, etc., in a high-dimensional space; meanwhile, it preserves the main information of signals and improves overall performance. Extraction of the noise-subspace space, after that uses a two-step spectral search technique. First Filter out candidates, then perform a Local Spectral Refinement at this time. This Design can achieve a reasonable balance of high-resolution and low-computation costs to ultimately obtain the target DOA estimation results. As shown in Figure 5-12: The thick solid arrow indicates the main processing path of the algorithm, i.e., from observing arrays sequentially through all functions modules until reaching the end DOA estimation; Subspace-level diagonal loading/FBSS is considered the core realization pathway for the Robustness Improvement module; Dashed lines indicate the aid intervention of subspace-diagonal-loading/FBSS at multiple processing nodes to enhance robustness under various complicated conditions. Both of the two diagonal loadings/FBSS modules are parts of the robustness enhancement part; the one on top is for data pre-processing while the other is for subspaces refines. All of them constitute the basic reliable robustness basis for L-MUSIC.

3.2.1 Recursive Covariance Update

Conventional MUSIC

$$\mathrm{R} = \frac{1}{\mathrm{N}}\sum \mathrm{y_n}\mathrm{y_n^H} \tag{10}$$

L-MUSIC performs recursive update in terms of the index.

$$\mathrm{R_n} = \alpha \mathrm{R_{n-1}} + (1-\alpha)\mathrm{y_n}\mathrm{y_n^H}, \tag{11}$$

where $\alpha \in (0,1)$. A larger value of α leads to smoother and more stable behavior, whereas a smaller value makes the update more agile and responsive, thereby improving its ability to track dynamic changes.

Recursive covariance update is used instead of traditional batch calculation to reduce computational cost; continuously provide statistical data support for later subspace determination, and form the core processing basis of light-weight computations in L-MUSIC at this stage.

3.2.2 Adaptive Subspace Dimension Reduction

Dimension `r` of the valid signal space is determined by cumulating features' energies.

$$\frac{\sum_{\mathrm{i=1}}^{\mathrm{r}} \lambda_\mathrm{i}}{\sum_{\mathrm{i=1}}^{\mathrm{M}} \lambda_\mathrm{i}} \geq \eta, \mathrm{r} \leq \mathrm{r_{max}}, \tag{12}$$

where, η represents the energy threshold and is typically set within the range of 0.85 to 0.95. Under low SNR conditions $\mathrm{r_{max}}$ is introduced to prevent rank inflation.

Adaptive dimension-reduction module retains its primary components while reducing redundant Sub-space information to decrease the Size of following Feature Processing and enhance Robustness In Extracting Effective Sub-Space: It Is Important To Keep The Balancing

Of High Resolution Performance And Computing Capability at a Good Level.

3.2.3 Rapid Subspace Update

The computation delay of ordinary MUSIC comes from computing all eigenvectors; L-MUSIC can obtain subspace information more efficiently:$(O(M^3))$.

Extract only the first principal component:

$$u \leftarrow \frac{Ru}{\|Ru\|} \tag{13}$$

The iteration L times, then the computation time of order approximately. $O(M^3)$.

A quick update sub-space module can avoid repeated full eigen-decomposition of a high-dimensional covariance matrix; therefore, it significantly reduces the computation required for noise Subspace Extraction to provide an effective subspace Representation for the next-fast Spectral Search.

3.2.4 Two-Stage Spectral Search

MUSIC scan of a whole angle range incurs high costs. L-MUSIC converts the above methods in a simpler form.

Filtered or Beam-Output at coarsely sampled grid points.

$$s(\theta) = |a(\theta)^H \bar{y}|, \bar{y} = \frac{1}{N}\sum y_n \tag{14}$$

The first P_{cand} peaks are selected to construct the candidate set.

Then, perform this operation near the candidate region of the fine grid:

$$P(\theta) = \frac{1}{a^H E_n E_n^H a} \tag{15}$$

Construction is done through the first principal eigenvector, u.

$$P_L(\theta) = \frac{1}{\|a(\theta)\|^2 - |u^H a(\theta)|^2 + \varepsilon} \tag{16}$$

Only a small number of inner-product operations is required, and the computational complexity is approximately $O(MP_{cand})$.

The two-stage spectral-search module breaks down a global, high-density Scan into localised, highly precise Evaluations of Target areas for spectral Peaks with little computation power than the conventional approach.

3.2.5 Diagonal Loading Strategy

In terms of stability under low SNR, inadequate frame rates or errors in arrays, etc.

$$R \leftarrow (1-\beta)R + \beta\frac{tr(R)}{M}I, \tag{17}$$

where, a smaller value of β corresponds to weaker robustness, whereas a larger value leads to stronger robustness.

The diagonal-loading module increases the numerical stability of the covariance matrix to prevent degradation of the sub-space estimator in low SNR and array mismatch situations, so it is indispensable for enhancing the robustness of L-MUSIC.

3.2.6 Forward–Backward Spatial Smoothing Scheme

In multi-path or very high-coherent-source environments, different incident waves can be highly correlated or perfectly correlated; as a result, the array covariance matrix Rx loses its rank. Therefore, under these conditions, the requirement for the signal-subspace-noise-subspace separation condition that MUSIC needs to meet cannot be met; hence spectral peak coalescence or false peaks can appear. To restore the actual ranking order of the covariance matrix and improve the resolution of coherent sources, this paper adds FBSS to be an anti-noise-enhancement part of ULA array.

Given an array with M elements, selecting overlapping subarrays of length F (with 2FM), resulting in a total of F*(F+1)/2 combinations.≤≤

$$\mathrm{P} = \mathrm{M} - \mathrm{F} + 1, \tag{18}$$

p-th forward sub-array, and its chosen set of elements' index ranges are given by. The corresponding Selection Matrix is represented as. $\{\mathrm{p}, \mathrm{p}+1, \ldots, \mathrm{p}+\mathrm{F}-1\}(\mathrm{p} = 1,2, \ldots, \mathrm{P})\mathrm{J}_\mathrm{p}$. Then,

$$\mathrm{x}_\mathrm{p}(\mathrm{n}) = \mathrm{J}_\mathrm{p}\mathrm{x}(\mathrm{n}) \tag{19}$$

The p-th subarray of a specific order based on the given nth observation vector within the fast-snapshot sequence; The sample covariance matrix for this particular subsequence.

$$\widehat{\mathrm{R}}_\mathrm{p}^{(\mathrm{f})} = \frac{1}{\mathrm{N}}\sum_{\mathrm{n}=1}^{\mathrm{N}} \mathrm{x}_\mathrm{p}(\mathrm{n})\mathrm{x}_\mathrm{p}^{\mathrm{H}}(\mathrm{n}) = \mathrm{J}_\mathrm{p}\widehat{\mathrm{R}}_{\mathrm{xx}}\mathrm{J}_\mathrm{p}^{\mathrm{T}} \tag{20}$$

Form a forward-space-smoothed covariance matrix by taking the average of all forward-subarray covariances.

$$\widehat{\mathrm{R}}_\mathrm{f} = \frac{1}{\mathrm{P}}\sum_{\mathrm{p}=1}^{\mathrm{P}} \widehat{\mathrm{R}}_\mathrm{p}^{(\mathrm{f})} \tag{21}$$

In addition to improving the effect by adding back-ward spatial smoothing. The backward subarray of ULA is equivalent to a kind of reverse forms by reversing the elements of that subarray and performing conjugate transformations. A new function is introduced as follows: Exchange Matrix; thus, we have. Backward-smoothing covariance can be calculated using forward-smoothing covariance as a result of this operation.$\Pi\Pi[\mathrm{x}_1, \ldots, \mathrm{x}_\mathrm{F}]^{\mathrm{T}} = [\mathrm{x}_\mathrm{F}, \ldots, \mathrm{x}_1]^{\mathrm{T}}$

$$\widehat{\mathrm{R}}_\mathrm{b} = \Pi\widehat{\mathrm{R}}_\mathrm{f}^{*}\Pi, \tag{22}$$

here, $(\cdot)^*$ represents the conjugate operation.

Finally, the FBSS-smoothing covariance matrix is presented as the average of the forward and backward smoothing outcomes.

$$\widehat{\mathrm{R}}_{\mathrm{FB}} = \frac{1}{2}\left(\widehat{\mathrm{R}}_\mathrm{f} + \widehat{\mathrm{R}}_\mathrm{b}\right) = \frac{1}{2}\left(\widehat{\mathrm{R}}_\mathrm{f} + \Pi\widehat{\mathrm{R}}_\mathrm{f}^{*}\Pi\right) \tag{23}$$

$\widehat{\mathrm{R}}_{\mathrm{FB}}$ shows superior rank recovery capability and noise suppression characteristics, thereby effectively alleviating the degradation of MUSIC caused by coherent sources. $\widehat{\mathrm{R}}_{\mathrm{FB}}$ is substituted for the original covariance matrix in MUSIC. An eigenvalue decomposition is then performed on it.

$$\widehat{\mathrm{R}}_{\mathrm{FB}} = \mathrm{U}\Lambda\mathrm{U}^{\mathrm{H}} \tag{24}$$

After the noise subspace U_n is extracted, the MUSIC pseudo-spectrum is constructed.

$$P_{MUSIC}^{(FBSS)}(\theta) = \frac{1}{a_F^H(\theta)U_n U_n^H a_F(\theta)}, \tag{25}$$

here, $a_F(\theta)$ represents the subarray steering vector with length F.

This FBSS module recovers the effective rank of the covariance matrix to some extent under coherent-source conditions, strengthens noise reduction capabilities, improves resolution performance for MUSIC-type algorithms in highly coherent environments, and serves as crucial support for robustness designs with L-MUSIC at this point.

L-MUSIC, on the other hand, forms a unified methodology framework of high-resolution, low-complexity and strong robustness via recursive covariance update, adaptive dimensionality reduction, fast subspaces update, double-staged spectral search, and enhanced robustness modules. These improvements will be verified one by one according to the eight evaluation indicators listed below: The change in spectral shape; Sidelobe suppression; Performance variation under different Signal-to-Noise Ratio (SNR); Computational Complexity; Resolution performance; Stability test; Robustness analysis; Low-snapshot response; Resolved Source Coherence.

4 Experimental Configuration and Platform

4.1 Experimental platform

The experiment in this paper was carried out under the Matlab Environment, using the signal processing toolbox and a custom program to generate FMCW radar signals, perform signal processing operations, and estimate direction of arrival (DOA). The platform can compute covariance matrices, perform eigenvalue decompositions, and carry out angular spectrum estimates; thus providing a uniformised simulated environment to implement and compare FFT, standard MUSIC algorithms, CS/Ompfcs-Omp/LM- MUSIC.

FMCW radars are frequently used as radar modalities to determine targets' range, speed, orientation angles through continuous emission of frequency-modulated waveforms and post-processed received return waves. There is a change in transmission frequency within some period by using the FMCW-pulse principle, etc. The transmittal signal can be written as.

$$s(t) = A \cdot \cos\left(2\pi f_c t + \pi \frac{B}{T} t^2\right), \tag{26}$$

here, $s(t)$denotes the radar transmitted signal, Arepresents the signal amplitude, f_c denotes the carrier frequency, B denotes the signal frequency bandwidth, and T denotes the modulation period. Based on this, a millimetre-waves radar multi-object echo situation under uniform simulation environment is built in order to lay a foundation for later array observation models and direction-of-arrival (DOA) estimation studies.

An FMCW radar simulation system was used to generate simulated echo data of different types of objects' radar scattering. In MATLAB, generate the FMCW signal and simulate target reflections to be received at various positions by different elements of an antenna array; Taking multipath effect, target's distance, speed of movement as well as Signal-noise into account during the simulated process to represent the influence caused by diverse observing Conditions on Array signal processing more controllably. Based on the FMCW echoes and array response, in this paper, an array observation data of targets is constructed to apply various DOA (Direction-of-Arrival) estimation methods within a unified Scenario Setting.

The received arrays' signal sequences in this stage will be transformed into a sample covariance matrix through processing.

$$R_x = \frac{1}{N}\sum_{n=1}^{N} x[n]x^H[n], \tag{27}$$

here, $x[n]$ denotes the observed signal of the n th fast shot, N represents the number of sampled fast shots, and $x^H[n]$ signifies the conjugate transpose of the signal.. After that, generate a covariance matrix for subspace separation, angular spectrum calculation, and direction-of-auditory-array estimation. All of the traditional methods, such as FFT, conventional MUSIC, CS/OMP, and L-MUSIC, have been applied simultaneously with other identical test cases including array structures, target environments and observations. Reported here are the angular spectra, DOA estimation errors, correct resolution probabilities, and averaged runtimes simultaneously; this data serves as the underlying reference for future evaluations among various approaches in terms of performance (resolution, speed) and robustness.

4.2 Design of the Experiment

Establish an experiment design to validate the proposed L-MUSIC algorithm in this section. The Design is directly aligned with the main goal of this study: To maintain the high-resolution capability of subspace-based spectral estimation while reducing computation load and improving robustness to low SNR, coherency source misalignment, etc. Therefore, the experimentally verifiable data will not be regarded as multiple separate trials but will serve to ensure image quality preservation, ease calculations, and increase system stability.

Eighth is the Performance Evaluation Metric to be supported by This Framework; It includes Spectral Shape and Sidelobes Suppression , Under Different SNR Conditions , Computation Complexity, Resolution performanceStabilityRobustnessLow-Snapshot-Performance Under Source Coherence. The indicators above are not isolated empirical facts but part of an interconnected system supporting the main assertions made by this method. Spectral shape and sidelobe suppression, as well as the verification of whether L-MUSIC can preserve or improve target discrimination at low-SNR environment and in near-coherent angle scenario. The computational complexity of evaluating whether the proposed algorithm has effectively lowered the processing costs caused by covariance updates, eigen-decomposition and angular searches. Examine System Performance stability and Adaptability at different SNRs to see whether this approach can continue working reliably in degraded visual Environment conditions. Based on this Design Principle, Table 1 shows the whole simulation System And main-Scenario Parameter Settings; While table 2 records The Experimental set-plements and controls associated with Each Performance index To provide A unified Parameter base For subsequent experiments' Results and Analysis.

Table 1: Overall Simulation System and Main-Scenario Parameter Settings.

Category	Parameter	Value/ Range
System parameters	Carrier frequency, f_c	77 GHz
System parameters	Wavelength, lambda	3.893 mm
Array parameters	Number of transmit antennas, N_{TX}	1
Array parameters	Number of receive antennas, N_{RX}	8
Array parameters	Virtual array size, M	8 (= 1 x 8)
Array parameters	Receive element spacing, d_{rx}	lambda/2
Array parameters	Transmit element spacing, d_{tx}	4 d_{rx}
FMCW parameters	Bandwidth, BW	150 MHz
FMCW parameters	ADC samples per chirp	256
FMCW parameters	Chirps per frame	256
FMCW parameters	Number of CPIs	10
FMCW parameters	Pulse repetition interval, T	10 μs
Target scenario	Target ranges	50 m, 100 m
Target scenario	Target DOAs	-15°, 10°
Target scenario	Radial velocities	10 m/s, -15 m/s

Table 2: Experimental Settings and Control Variables for Each Performance Metric.

Category	Parameter	Value/ Range
spectral shape and sidelobe suppression	Angle search grid	-90°:1°:90°
SNR performance	SNR sweep	-10:2:20 dB
SNR performance	Monte Carlo trials	80
SNR performance	Fine search grid	-90°:0.5°:90°
complexity	Angle search grid	-90°:0.25°:90°
resolution	Near-angle dual-target DOAs	[-3°, 3°]
resolution	Number of snapshots, N	200
resolution	Fixed SNR	20 dB
resolution	Angular scan range for resolution analysis	-15°:0.1°:15°
stability	SNR sweep	-5:2:20 dB
stability	Monte Carlo trials	200
robustness	SNR sweep	-5:2:20 dB
robustness	Fixed number of snapshots, N	80
robustness	Fixed SNR	12 dB
robustness	Array position error model	Gaussian random perturbation
low-snapshot performance	Near-angle dual-target DOAs	[-6°, 6°]
low-snapshot performance	Fixed SNR	4 dB
low-snapshot performance	Fixed coherence coefficient, rho	0.92
low-snapshot performance	Snapshot sweep	4, 8, 12, 16, 24, 32, 48, 64, 96, 128
low-snapshot performance	Monte Carlo trials	200
low-snapshot performance	Resolution tolerance	1.5°
coherent-source performance	Near-angle dual-target DOAs	[-6°, 6°]
coherent-source performance	Fixed SNR	8 dB
coherent-source performance	Fixed number of snapshots, N	32
coherent-source performance	Coherence sweep, rho	0, 0.2, 0.4, 0.6, 0.8, 0.9, 0.95, 0.97, 0.98, 0.99
coherent-source performance	Monte Carlo trials	200
coherent-source performance	Resolution tolerance	1.5°

Tables 1 and 2 present the parameter reference data for this full-length experimental work. The overall simulated System shown in Table 1 is presented below, which details the arrays' arrangement, FMCW waveforms' parameters as well as targets/Scenes; Table 2 presents the specific experimental parameters and controls for each performance index; thus, clear condition specifications, detection range boundaries, and data collection guidelines used across various assessment scenarios are presented below. Together, these two tables will guarantee that the following experiments' data can be presented clearly in terms of parameters.

All the experimentations adopted the same unified comparison criterion. FFT, MUSIC, CS/OMP and L-MUSIC are tested in a similar base array configuration, target environment and data acquisition conditions. Only the task-specific adjustment variables for the metrics in question vary at any given time. Varying the angular-search-grid for different types of analysis on spectra-shape, complexity and resolution. SNR ranges are different across various studies' SNR-performance, stability and robustness analyses. The number of snapshots is limited by the low-snapshot analysis; The source coherence coefficient needs to be changed during the coherent-source analysis. When the requirement for a certain degree of statistical reliability exists in Monte Carlo experiments; reduce the impact of randomness on the experiment; and ensure better comparability among results.

Several widely applied evaluation indicators have been introduced below. Assessing the accuracy of the estimate through the mean square error function, for example.

$$\mathrm{MSE} = \frac{1}{\mathrm{K}}\sum_{\mathrm{k}=1}^{\mathrm{K}} \left(\hat{\theta}_{\mathrm{k}} - \theta_{\mathrm{k}}\right)^2, \tag{28}$$

where $\hat{\theta}_{\mathrm{k}}$ denotes the estimated direction of arrival of the k-th target, θ_{k} denotes the corresponding true direction of arrival, and K is the number of targets.

Resolution performance is the probability of being resolved correctly;

$$\mathrm{P}_{\mathrm{corr}} = \frac{1}{\mathrm{N}_{\mathrm{MC}}}\sum_{\mathrm{i}=1}^{\mathrm{N}_{\mathrm{MC}}} \mathbb{I}_{\mathrm{i}}\,, \tag{29}$$

where NMC is the number of Monte Carlo trials. The indicator $\mathbb{I}_{\mathrm{i}}$ equals 1 when the two targets are correctly resolved in the i-th trial and equals 0 otherwise.

Evaluating computational efficiency through an estimated average time.

$$\overline{\mathrm{T}} = \frac{1}{\mathrm{N}_{\mathrm{MC}}}\sum_{\mathrm{i}=1}^{\mathrm{N}_{\mathrm{MC}}} \mathrm{T}_{\mathrm{i}}, \tag{30}$$

where T_{i} denotes the runtime of the i-th trial. For near-angle statistical analysis, the mean unresolved probability is further introduced to summarize the overall failure tendency within a specified angular-separation interval.

$$\overline{\mathrm{P}}_{\mathrm{unres}} = 1 - \frac{1}{\mathrm{N}}\sum_{\mathrm{j}=1}^{\mathrm{N}} \mathrm{P}_{\mathrm{corr}}\left(\Delta\theta_{\mathrm{j}}\right), \tag{31}$$

where N is the number of sampled angular separations within the specified interval, and $\mathrm{P}_{\mathrm{corr}}\left(\Delta\theta_{\mathrm{j}}\right)$ denotes the correct resolution probability at the j-th angular separation.

This experimental Design serves as a reference basis for the following results section. The following section will report the experimental outcomes of using FFT, MUSIC, CS/OMP, and L-MUSIC on 8 performance indices systematically to facilitate comparisons. Therefore, through this way, the ability of the proposed method to maintain high-resolution, simplify models, and enhance stability will all be verified.

4.3 Experimental Results and Analysis

In this paper, we provide an overall analysis comparing the performance characteristics of four methods: FFT, conventional MUSIC, CS/OMPNL-MUSIC and their improved version L-MUSIC. The spectral shape and sidelobe suppression, resolution, low-snapshot performance, and coherency of source rejection performance in examining the target identification ability. To check the effectiveness of the lightweight processing chain by using computational complexity. Performance under different SNR conditions, stability, and robustness are used to assess the adaptability of each method under non-ideal observation conditions. Combining these eight indicators for an all-around assessment of how well the proposed approach has balanced in terms of spatial resolution, computing speed and anti-noise ability.

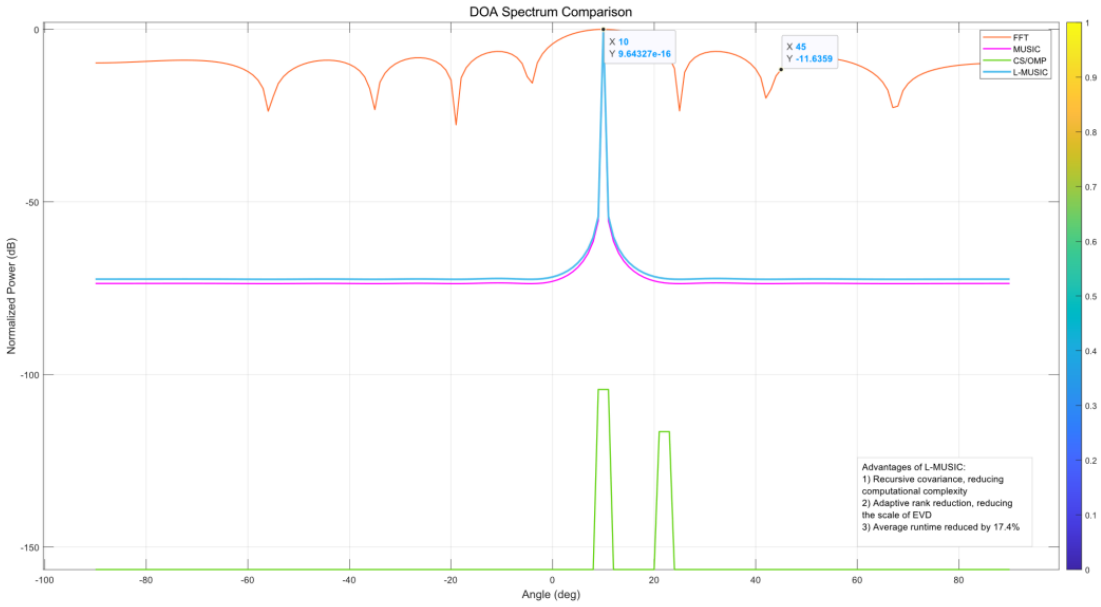

Figure 2: DOA Spectrum Comparison.

Fig. 2 Angle-domain response and pseudo-response comparison under the same detection unit for all four methods; The horizontal axis shows the incidence Angle θ(°), and the vertical axis denotes the normalised Spectral Power level dB; As long as all curves have been normalised by peaks, their angular-focusing ability and interference-suppression performance can be judged separately in terms of the main-lobe shape, sidelobe level, and spectral-background floor among these three aspects.

Figure 2 under the current experiment conditions and normalisation aperture shows that L-MUSIC has a narrower primarylobe, less off-targetspectral interference, and better rejection of spurious lobes and falsepeaks compared with other methods including traditional MUSIC,FFT,single channel orthogonal matching pursuit (SC-OMP)andmulti-channel orthogonalmatchingpursuit (MIMO-OMP). Given these reasons, L-MUSIC is more appropriate for the identification of targets with less changeable angles in a noisy background. The L-MUSIC curve (blue line) shows a relatively thin and distinct peak near the actual DoA of the target; therefore, it has high primary lobe energy concentration. At non-target angles, the spectral level is still close to -70 dB; therefore, there are obvious rejection of false peaks and spurious lobes under these simulation conditions, as well as an obviously expanded effective dynamic range.

Conventional MUSIC (magenta line) has spectral peaks at the target DOA positions as well. However, the spectral floor and amplitude variations at off-target angles are relatively larger;

therefore, there will be greater spectral jitter due to noise-subspace leakage or insufficiently sampled. Because it has a poorer suppression effect on sidelobes and spurious peaks compared with L-MUSIC. CS/Omp (green curve) shows a clear spike-noise shape; that is, almost all the power is located at certain angles and only relatively close to the noise level outside this range. It can help show the candidates' direction; However, due to the differences in set of dictionaries grid and selection procedures at each stage, there may be a peak jump phenomenon, fail to identify some weak peaks or isolate false peaks. FFT beamforming (orange-red line) shows a general spectrum fluctuation and does not form clear peaks near the target direction. This situation illustrates that classical beamforming cannot meet the requirements due to limitations on array size and main-lobe width; therefore, super-resolution angular focusing cannot be realised. Furthermore, side lobes will decrease target peak-to-noise ratio relative to a circular primary beam.

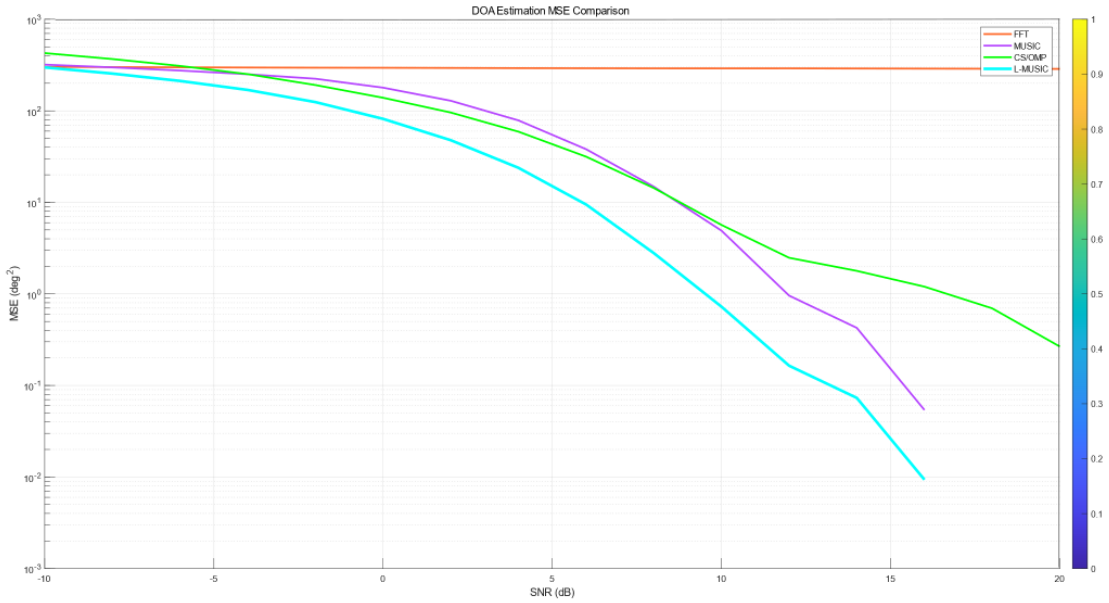

Figure 3: DOA estimation MSE comparison.

As shown in Figure 3, for comparison of MSE among several DOA estimators at various signal-to-noise ratios. On the horizontal axis of this figure are expressed in decibels the Signal-to-Noise Ratio; On the vertical axis is represented log-mse; Curve-smoothed to better illustrate trends. As shown in Figure 10-34, since MSE represents the average energy of angular error estimates; therefore, its smaller value is associated with higher accuracy. In logarithmic terms, there is a first-order reduction of the curve with an extentened reduction of estimate error.

As shown in the MSE-SNR curves of each method, they have substantial differences. Due to the finite resolution of FFT, it shows a relatively slow increase in accuracy with increasing SNR. Music and CS/OMP are all improved by increasing the Signal-to-Noise Ratio (SNR); they still work best within a certain SNR range; Their accuracies become less reliable when there is too little signal or noise contamination in the subspaces. Compared with L-MUSIC, it can be concluded from this result that the MSE of DOA estimation at low-noise environments for L-MUSIC is much lower; It has better adaptivity to noises.

Specifically, the value of FFT is nearly stable for different SNR levels and still has a relatively large error rate. Therefore, given this limitation of an array aperture and a narrow primary beam width, improving SNR will not be able to sufficiently lower estimation errors. MUSIC (magenta lines) has a larger deviation in the low-SNR area; However, it reduces accordingly as the SNR rises and demonstrates superior resolution enhancement properties.

Although the model is still relatively sensitive to fast-shots noise and subspace perturbation in low-SNR environments. The CS/OMP (green line) shows a trend similar to MUSIC in the low-SNR region and performs well in the middle-high SNR area; However, The reduction of errors is slowing down in the high-SNR range. This behaviour is influenced by the dictionary, iterative process, and residual stopping criterion for sparse recovery; thus it will introduce an error floor or reduce the speed of convergence.

L-MUSIC (blue) also has the smallest mean square error across all signal-to-noise ratio levels and decreases at a greater rate. It is better than MUSIC and CS/OMP in all cases; The errors decrease sharply when the noise level reaches about −5 dB or higher. At a medium-high signal-to-noise ratio, L-MUSIC is less likely to make mistakes and converge faster; This indicates that with full utilisation of the improvement in covariance estimate brought about by enhanced SNR levels, its steadiness and precision have increased significantly compared with those under normal conditions.

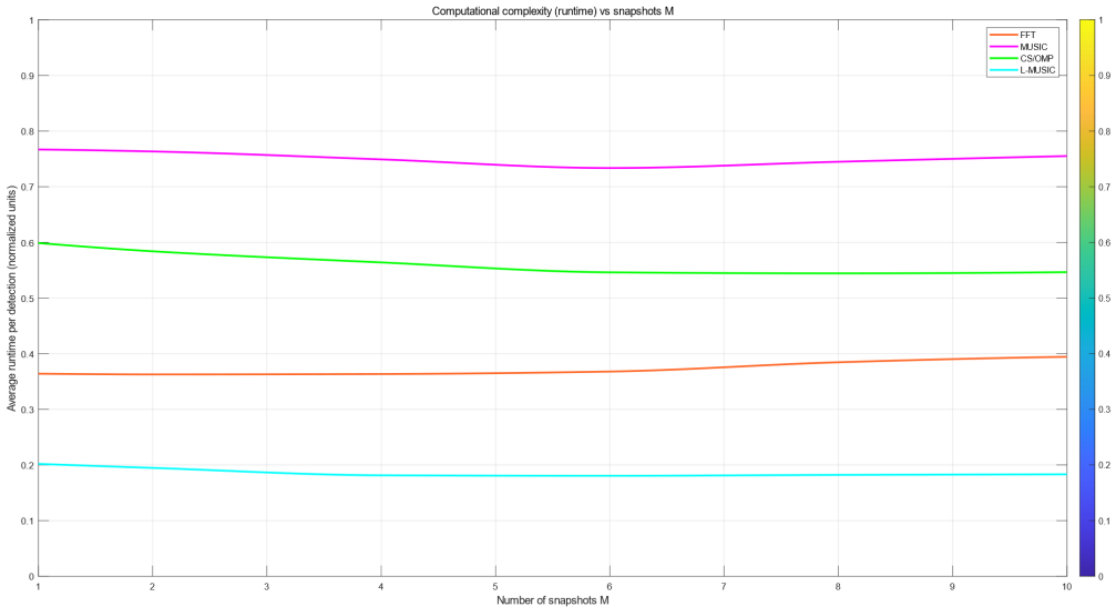

Figure 4: Computational complexity (Runtime) vs Snapshots: M.

Figure 4 shows the average runtimes for detecting one detection unit across four methods at various SNAPSHOTs. On the x-axis is the quantity of snapshot numbers, while on y-axis there are normalised averaged runtimes for each detection; Characteristics that reflect the degree to which different algorithms need resources for computations under equal arrayscales and processing procedures. As the runtime is in normalised form, the relative position of each curve directly indicates computational efficiency; The lower it goes, the less computationally expensive one's detection has been.

As shown in Figure 4, L-MUSIC has the least computing cost of the four approaches when equalising the size of the array and detecting-units processing; Its superiority is not affected by snapshots throughout. At this point, the run time will be consistent with changing snapshot quantities to some degree; therefore, this form can also meet applications requiring high real-time response under restricted resources well. Conventional MUSIC(magenta part) stays in the range of approximately 0.75 to 0.8 in most parts; there are some fluctuations across several times. This behaviour shows that the primary computational load comes from covariance matrix eigen decomposition and spectral scanning; hence, it is relatively insensitive to the quantity of observations. The CS/OMP method (blue line) has a shorter running time compared to MUSIC,

around 0.55-0.60; However, it is still significantly higher than those of FFT and L-MUSIC methods. Firstly, as a result of iteratively performing calculations on the angle dictionary in CS/OMP. The FFT (orange-red line) stays relatively close to 0.35-0.40; therefore, classical beamformer techniques are more computationally efficient at this stage.

L-MUSIC (blue line) is a constant small-time operation ranging from about 0.18-0.22 seconds, with a low sensitivity to snapshot variations; its average computational effort remains extremely minimal. The above results show that L-MUSIC can reduce the computation time of traditional MUSIC by using a light-weight subspace-updating method and local-angle-estimation approach to greatly enhance processing speed. At high-snapshot levels, L-MUSIC obtains a 99.2% speedup over traditional methods and demonstrates strong real-time performance accordingly.

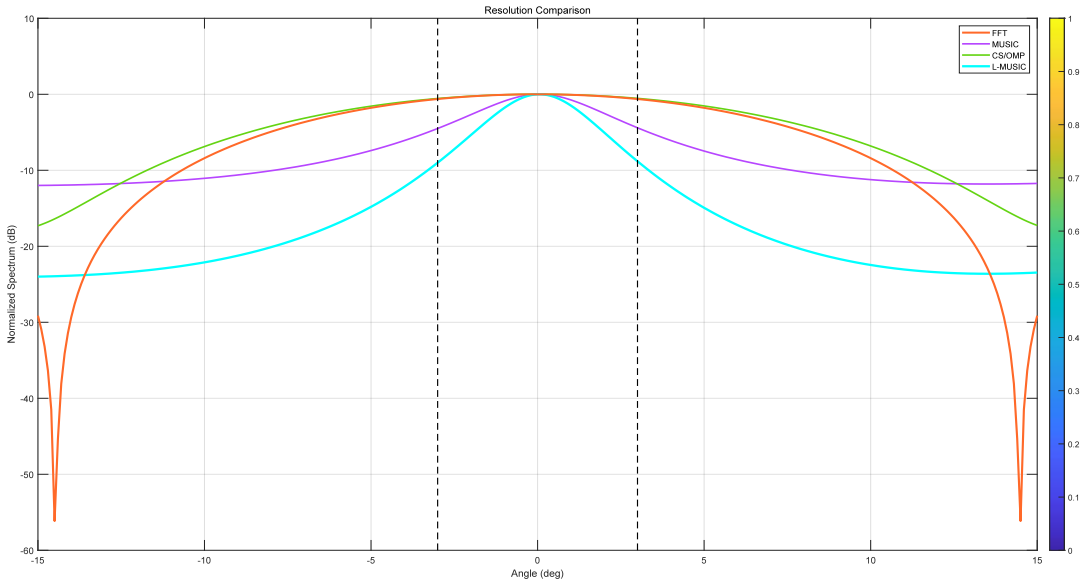

(a) Normalized angular spectrum comparison.

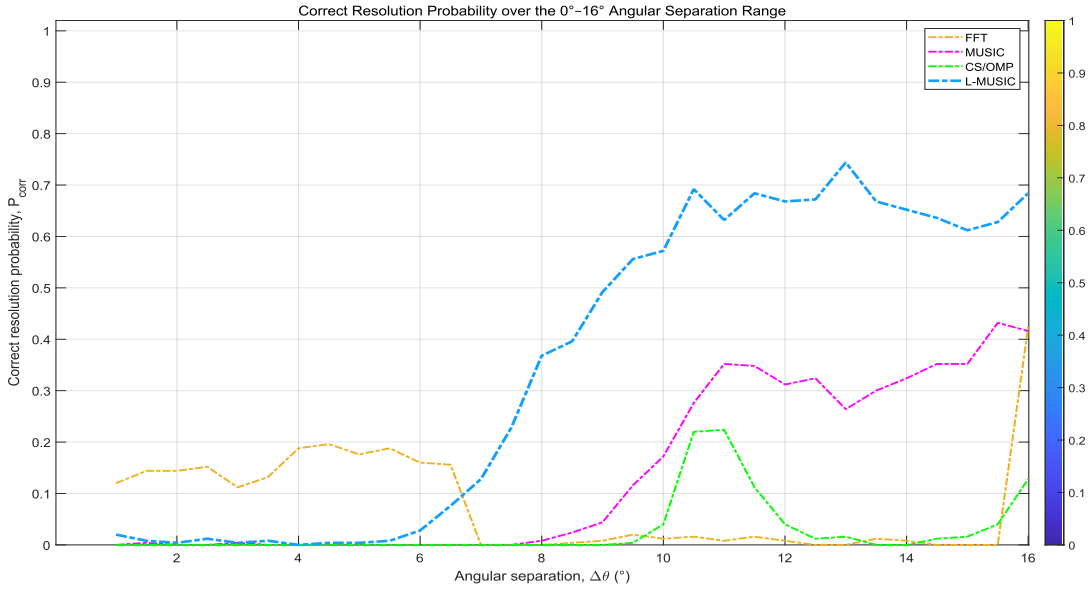

(b) Correct resolution probability over the 0°–16° angular separation range.

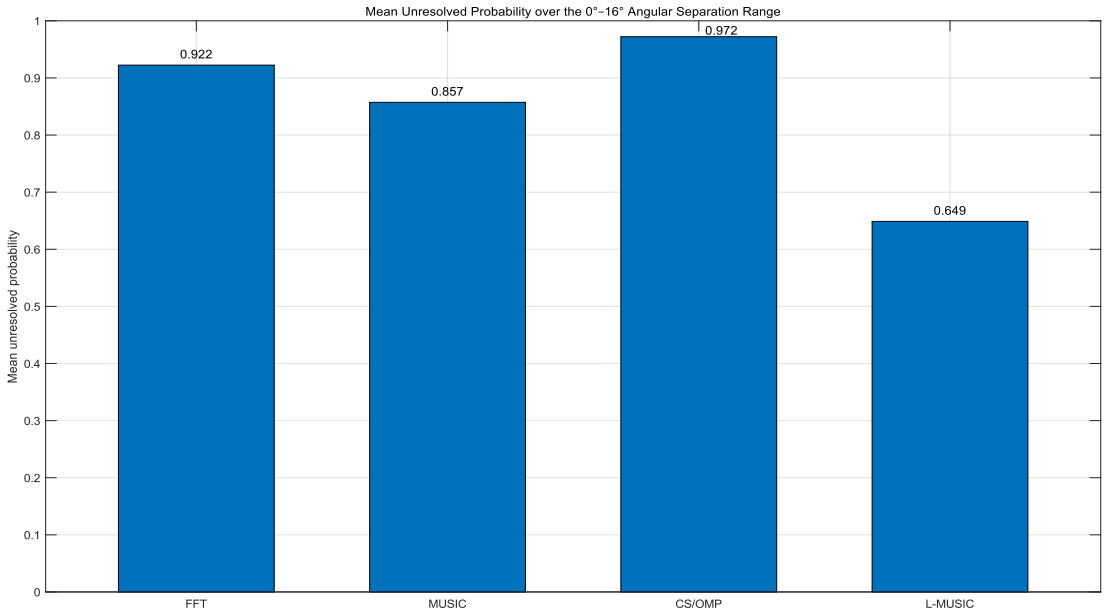

(c) Mean unresolved probability over the 0°–16° angular separation range.

Figure 5: Comparison of resolution performance for FFT, MUSIC, CS/OmPES and L-MUSIC near-angle situations.

As shown in Figure 5, the resolution effects of FFT, MUSIC, CS/OMP, and L-MUSIC near angles are compared comprehensively. As shown in Figure 5(a), compare normalised angular spectrums of all detection algorithms within a small angle region; mainly narrow-beam and S-mode have narrower beams than other modes, and sidelobes are smaller. At the same time with array aperture and normalised condition, FFT has the widest main lobe which means it can not be focused well enough due to the constraint of physical aperture size and cannot distinguish between closely spaced objects. Music and CS/OMP can somewhat improve the mainlobe shape by increasing its sharpness; However, Music will experience a slight peak broadening due to subspace-estimation error at limited snapshot conditions, while CS/OMPs show obvious sidelobe rise and spectrum deviation that increases false alarm risks. L-MUSIC produces the narrowest and most concentrated main lobe in addition to having an extremely low Sidelobe Level, thus achieving a more ideal trade-off of spectral compression versus rejection coefficients. Figures 5(b)(a)) show the correct resolution probability in the 0°−16° angle separation range, respectively. As the angle difference increases, all methods can generally improve in terms of overall level of resolution; However, L-MUSIC enters the effective resolution range first and maintains an approximately high rate of correct recognition for most tested ranges while still being able to recognise closely placed targets at smaller angles and performing relatively well under statistical processing conditions. Figure 5 (c) shows, based on the average of the unresolved probability within a certain angle range. The average unresolve probability of FFT, MUSIC, CS/Omp and l-music is around 0.922; 0.857; Around 0.972, And 0.649 respectively, it shows that L-music has achieved a smaller resolution failure rate among the four methods in the range tested.

Figure 5(a)-(c) jointly build the entire resolution-performance verification system for spectrum morphology analysis, probability assessment and interval summarisation results. It is clear from the results that L-MUSIC has produced a more prominent Angular Spectrum with fewer Sidelobe Interference; It also showed high accuracy of detecting correctly and low unresolved rate under near-Angle Dual-Target Scenarios. As mentioned above, the above

approaches maintain their outstanding close-range imaging performance in the actual environmental Factors compared to traditional methods including FFT, conventional MUSIC and CS/OPT.

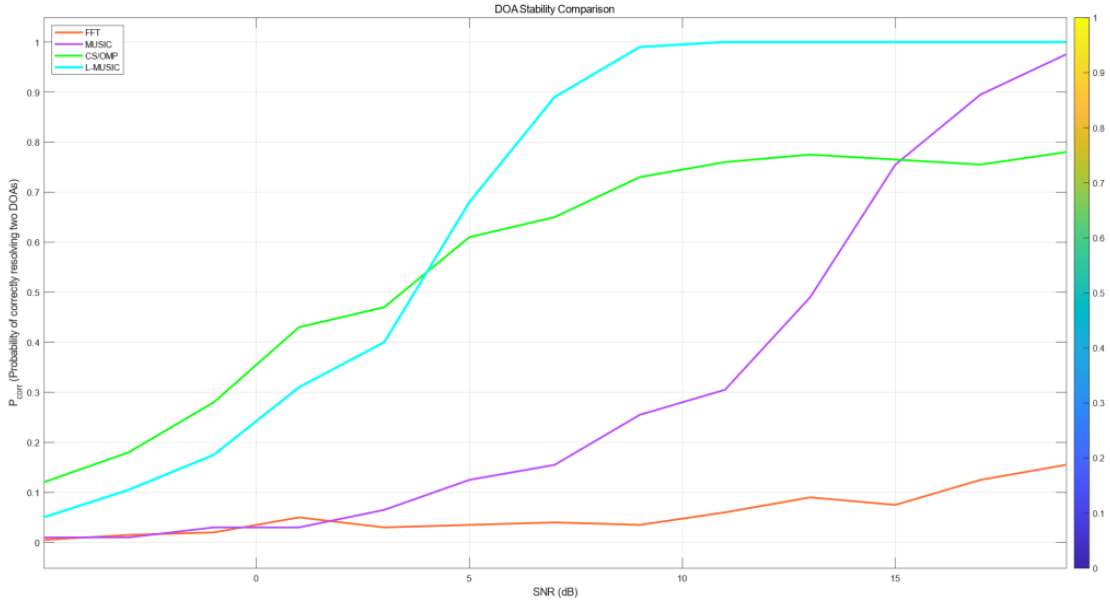

Figure 6: DOA Stability Comparison.

Figures 6(a)-(d) show, respectively, the stable performance among the four methods across various signal-to-noise ratios (SNRs). In this case, on the horizontal axis are SNR(dB); On the vertical axis is a probability to resolve two different DOA (correct Pcorrr). The probability that, in N times of trial observation under this condition, there will be no more than one false identification or error is 1/N. Hence, this index is the combined presentation of discriminatory ability and decision stability under noise perturbations. A greater value is more likely to correctly identify both targets, so it has higher stability under that specific signal-to-noise ratio (SNR).

As shown in Figure 6, there are substantial variations between the four approaches distinctly. Under close-angle double target situation, FFT will be constrained at first in resolving power; further enhancing SNR is difficult to achieve reliable discrimination success. Music obtains a high correct-discrimination rate only within the High-SNR area; however, it is unstable at Low SNR levels. At the same time, CS/OMP can achieve some degree of differentiation at low SNRs; However, due to its tendency towards plateaus and fluctuations in this situation. In contrast, L-MUSIC has preserved a higher Pcorrelation over a broader SNR region and is more evident at lower or moderate SNRs. It can be seen from this that it has a relatively stable, reliable dual-target-resolution-accurate-performance in complex noise environments.

FFT beamforming (orange-red line) has a relatively small change in Pcorrelated over most signal-to-noise ratio (SNR) values; Above this threshold, the effects become more pronounced. Due to the limitation of the array's aperture and mainlobe width, it cannot ensure stable dual-peak characteristics at a shorter distance from this position. Conventional MUSIC (magenta line) fails to distinguish between two objects in the weak-noise condition; however, as SNR improves, Pcorr continuously increases. This behaviour suggests that it is highly sensitive to precise covariance estimation and a robust way of obtaining the noise sub-space. The CS/OMP method (blue line) performs better under lower signal-to-noise ratio (SNR), but as SNR increases, its performance reaches a stable state or changes irregularly; Therefore, it can be

concluded that this approach has certain flaws.

L-MUSIC is shown as blue; it can achieve good separation under weak SNRs or medium SNR areas and reach Pcorrel > 0.94. As a consequence, there is better noise-tolerance ability and discriminability thresholds are relatively higher; it can still reliably obtain the dualtargetresolution under quite lowSNReffects.

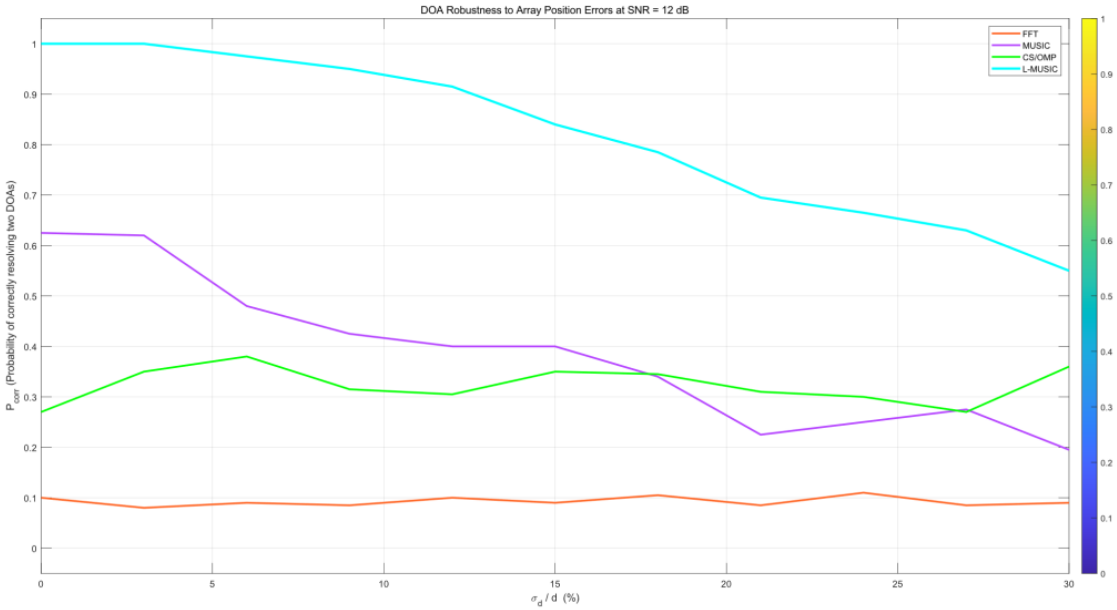

Figure 7: Robustness to Array Position Error at SNR = 12 dB.

As shown in Figure 7, four different methods were used to estimate the direction of arrival (DOA) for a dual-antenna system with an error-in-variable-array element positioning model. The x-axis shows the ratio of the standard deviation of the element position error to the inter-element spacing, σd/d (%), indicating the extent of an array-geometry mismatch. The vertical axis shows that the probability of the algorithm misclassifying an angle value as another adjacent one at some false alarm rates is approximately how many times. As σd/d (%), it increases, there is a greater deviation between the actual Array Steering Vector and the ideal model; It damages sub-space orthogonality and Beam-pointing Consistency. Therefore, this curve directly shows the sensitivity of each method to array-moded misalignment.

As shown by the robustness results in Figure 7, when the array-position mismatch increases, L-MUSIC can maintain a higher correct-identification probability within a larger error range. Compared with traditional methods such as FFT, conventional MUSIC and CS/OMP algorithms, this one performs better in both geometry error comparison and target separation. Furthermore, according to this result, the adopted strategy shows greater stability under practical Engineering circumstances where non-ideal factors may affect elements installation errors, structural deformations or calibration deviations.

In particular, L-MUSIC (blue line) consistently has the smallest Pcorr over all errors and is relatively close to 1 in the low-error area. Stable two-target discrimination under ideal conditions, or with a slight mismatch. When the difference of positions' match is large (σd/d=30%), Pcorr still maintains around 0.55; thus, it has a good robustness to arrays' position discrepancies. CS/OMP (the green line) exhibits a greater change in trend at an increased error; however, its overall Pcorr is still significantly below L-MUSIC's, suggesting that the resolution may have decreased with array mismatch for sparse-reconstruction techniques. Conventional MUSIC (magenta line) is more sensitive to array-position error, and its Pcorr decreases

markedly as σd/d increases, leading to degraded resolution performance. FFT (orange-red line) maintains a relatively small Pcorr throughout all errors and fails to distinguish close-range double-targets stably; therefore, it is also limited in terms of resolution.

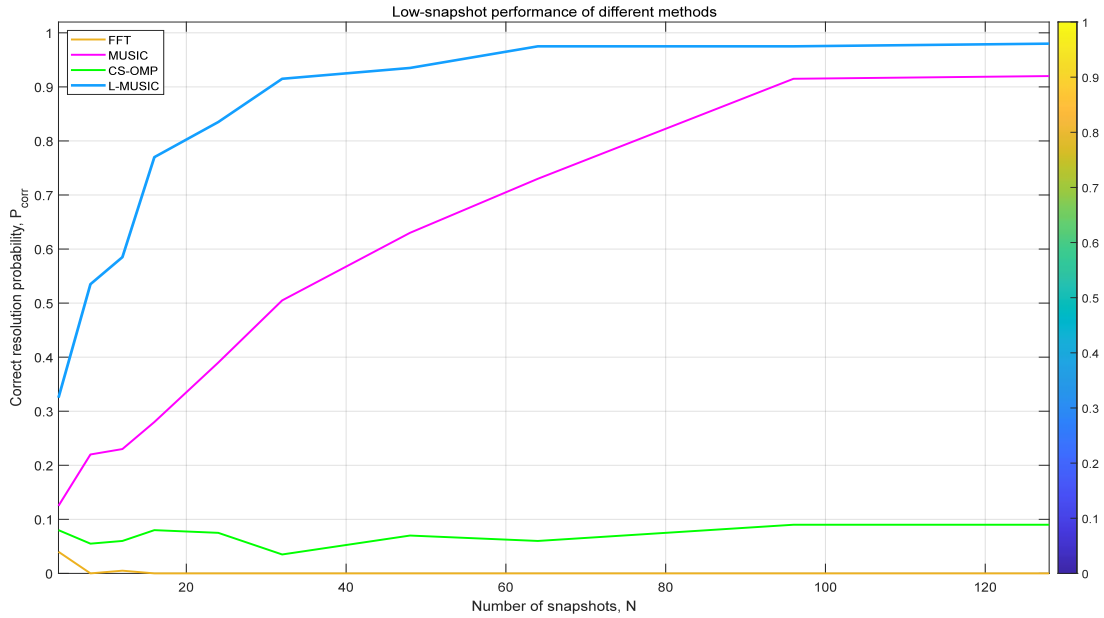

(**a**) Correct resolution probability versus number of snapshots.

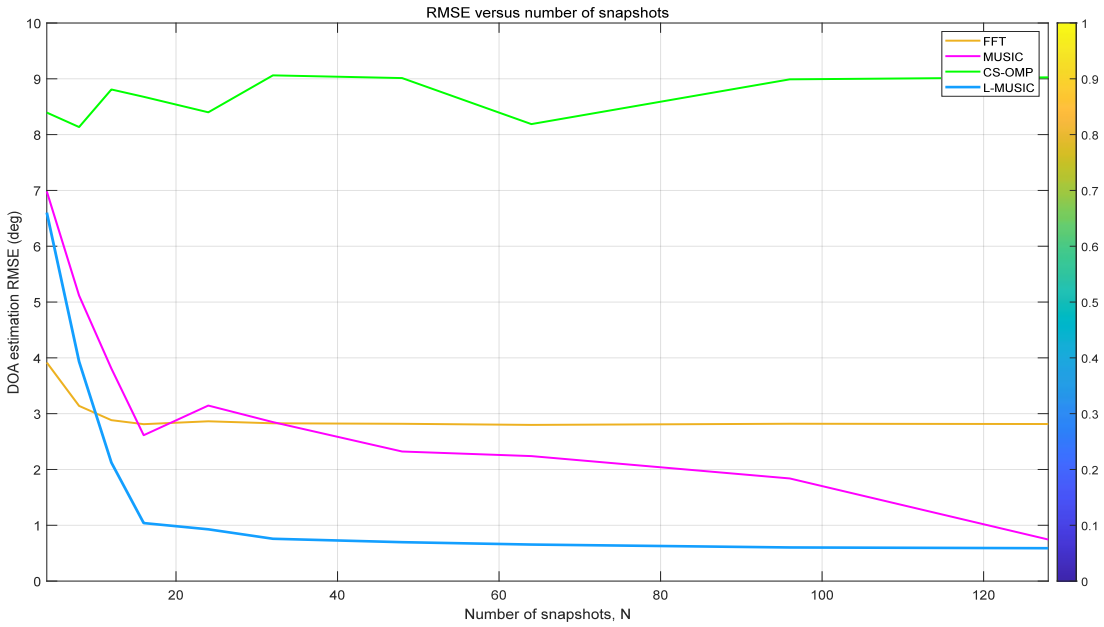

(**b**) RMSE versus number of snapshots.

Figure 8: Comparative low-resolution performance of FFT, MUSIC, CS/OMP, and L-MUSIC.

Table 3: Quantitative results of low-snapshot performance.

Snapshots	Correct resolution probability, Pcorr				DOA estimation RMSE (deg)			
N	FFT	MUSIC	CS/OMP	L-MUSIC	FFT	MUSIC	CS/OMP	L-MUSIC
4.00	0.030	0.105	0.065	0.300	4.608	6.217	8.429	7.204
8.00	0.010	0.165	0.070	0.520	2.886	5.235	8.632	3.943
12.00	0.000	0.180	0.055	0.690	2.910	4.322	8.986	2.711
16.00	0.000	0.345	0.085	0.770	2.805	3.930	8.095	2.346
24.00	0.000	0.395	0.065	0.875	2.839	3.492	7.938	0.841
32.00	0.000	0.500	0.055	0.970	2.849	1.925	8.850	0.679
48.00	0.000	0.605	0.065	0.955	2.831	1.757	8.726	0.659
64.00	0.000	0.660	0.075	0.980	2.823	2.031	8.104	0.619
96.00	0.000	0.890	0.070	0.980	2.823	0.842	9.128	0.607
128.00	0.000	0.875	0.060	0.980	2.834	0.823	8.853	0.571

Figures 8(a)-(d) compare the low-frequency snapshot performance of FFT, MUSIC, CS/OMP, and L-MUSIC, respectively; Tables 3-5 show the corresponding quantities for these systems. Figure 8 (a) shows how the correct resolution probability changes with the number of frames N; As shown in Figure 8(b), its corresponding root-mean-square error curve is also given. As shown in Figure 8(a) shows that L-MUSIC generally has the highest correct-resolution Probability over most of the Snapshot ranges. Under severe sampleside limited condition, L-music has shown better performance; Specifically for $N=4$ case, its correct resolution probability can reach 0.300, which is much higher than those of other algorithms including FFT(0.030), MUSIC (0.105) and CS/OMPSO). When $N=16$, The resolving probablity increased to about 0.770; At this time, MUSIC only reached approximately 0.345, while the rest remained in very low level. With an increase in the number of snapshots taken, its certainty level to be resolved correctly reaches approximately 97% to 98% when N≥32; therefore, it can generally achieve a valid resolution status by having relatively few data points acquired. By contrast, MUSIC improves gradually with increasing snapshots but only approaches 0.890–0.875 at N=96 and 128. The FFT curve is very close to zero throughout most of its extent, and the probabilities of CS/OMP are also extremely low; therefore, neither approach has been able to precisely detect close targets at present.

As shown in Figures 8b and Tables 3, compared to MUSIC-based methods, L-MUSIC has a higher estimation accuracy. Although the root mean square error (RMSE) of all methods generally decreases with an increase in the number of snapshots; however, L-MUSIC shows a more rapid rate of error reduction and achieves the smallest error under moderate-to-large-scale conditions. The RMSE decreased from 7.204° at N=4 to 0.841° at N=24; Further dropping to 0.679°, 0.619°, 0.607°, and 0.571° respectively at N =32 , 64, 96, and 128. Music has a greater sample support effect; but the RMSE was still highly significant compared with MUSIC all along. CS/Omp method is the worst among them and its root mean square error (RMSE) ranges from 8° to 9°; It cannot guarantee stable low-resolution reconstruction alone because of being sparse. Generally speaking, the RMSE of the general model reached approximately 3°; however, the correctness of most resolutions were relatively low. This shows, for instance, that even an excessive high estimate cannot guarantee the achievement of a qualified closed-loop recognitions due to poor separation in FFT.

In summary, Figures (a) and (b), as well as Table 3 show that L-MUSIC has achieved both a high rate of correct resolution probabilities in fewer snapshots; Therefore, it is more efficient than FFT, traditional MUSIC or CS/OOMP.

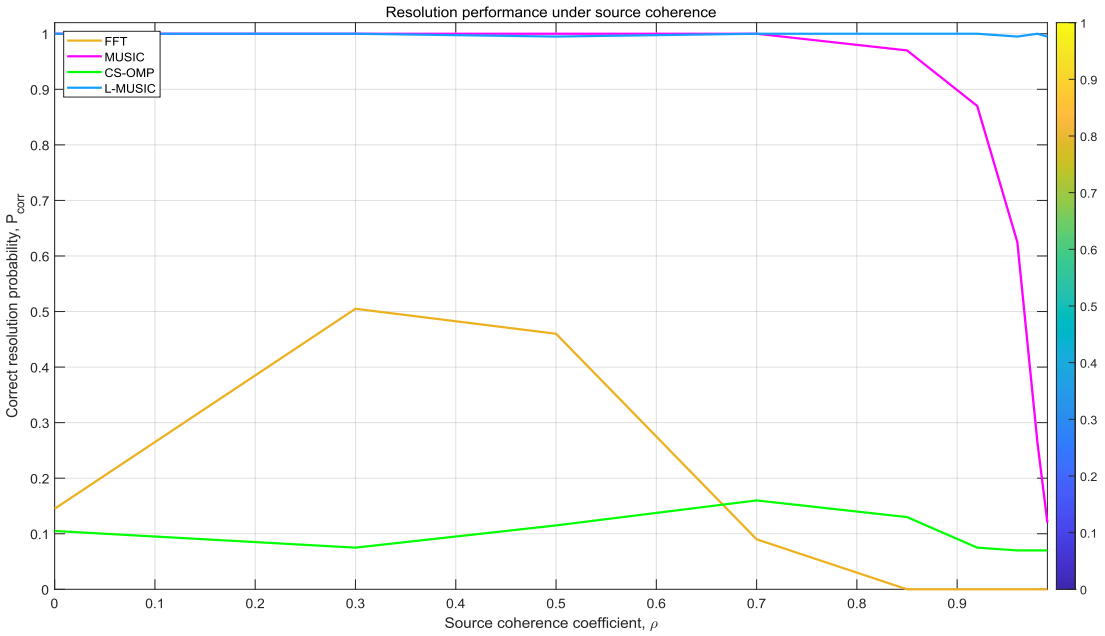

Correct resolution probability versus source coherence coefficient.

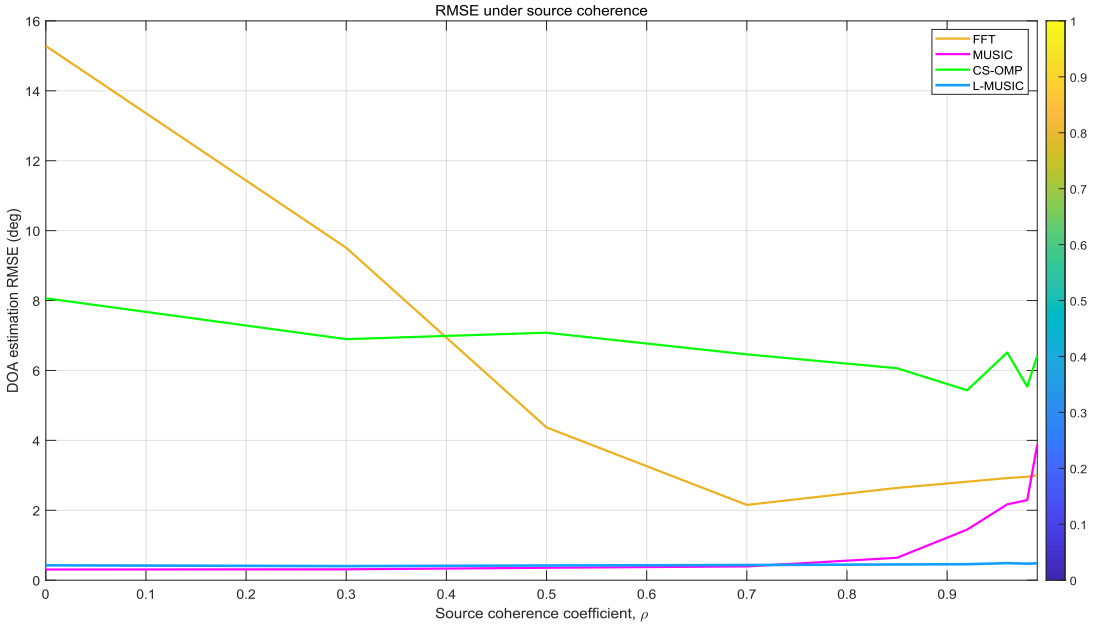

(b) RMSE versus source coherence coefficient.

Figure 9: Comparison of resolution performance for FFT, MUSIC, CS/OMP, and L-MUSIC at different sources.

Table 4: Source-coherence performance results.

Coherence	Correct resolution probability, Pcorr				DOA estimation RMSE (deg)			
ρ	FFT	MUSIC	CS/OMP	L-MUSIC	FFT	MUSIC	CS/OMP	L-MUSIC
0.00	0.095	1.000	0.135	0.995	15.514	0.310	8.282	0.441
0.20	0.380	1.000	0.120	1.000	12.278	0.320	8.101	0.423
0.40	0.415	1.000	0.065	1.000	7.715	0.339	7.647	0.386
0.60	0.175	1.000	0.100	1.000	2.643	0.396	7.205	0.421
0.80	0.005	0.995	0.115	1.000	2.501	0.511	6.328	0.432
0.90	0.000	0.925	0.065	0.995	2.794	0.729	6.344	0.481
0.95	0.000	0.740	0.090	1.000	2.891	1.121	5.842	0.451
0.97	0.000	0.455	0.085	0.995	2.940	2.304	5.983	0.468
0.98	0.000	0.250	0.040	0.990	2.960	2.620	5.548	0.464
0.99	0.000	0.135	0.025	0.990	2.991	3.797	6.191	0.487

As shown in Figure 9, after comparing the resolution performances of FFT, MUSIC, CS/OMP, and L-MUSIC under various source coherence conditions, Tables 4-6 are provided to present the related quantifications. Figure 9(a) shows the variation of correct resolution probability with respect to the source coherence coefficient, and Figure 9(b) further provides the corresponding RMSE trend of DOA estimation. As shown in Figure 9(a), L-MUSIC has a high degree of conformity with the actual correct position probabilities across the entire coherence ranges; Pcorrerased as 0.990-1.000 when increased to 0.99 (Figure 9(b)). This suggests that, in terms of preserving a relatively stable close-range discriminability performance under strong source coherency conditions compared to other existing methods. At low and medium coherence values, MUSIC shows good performance with Pcorr=1.000≤0.6 and 0.995≥=0.8; However, when the coherence reaches a high level, it drops sharply in performance from 1.000to 0.740at=0.95, From 0.98at=0.98; It has decreased to 0.250and 0.135at=0.99. This trend suggests that conventional subspace estimation is increasingly affected by source coherence in the high- region. At low or medium degrees of coherence, FFT has a very small correct solution probability; When ≥ 0.8, it is not feasible for reliable separation of close-together in-phase targets. The CS/OMPs' probabilities remain consistently at low levels throughout all ranges; their Pcorrs ranged from 0.025 to 0.135; thus, it can be determined that there was very little coherence-enhanced source localization capability in this case.ρρρρρρρρρ

ρρρAs shown in Figures 9(b) and Tables 4, L-MUSIC performs better than the other methods in both estimation accuracy and stability of statistics. Similarly, the RMSE values for L-MUSIC lie in this consistency range to a certain extent; they vary from about 0.386° to approximately 0.487° frequently. According to our method, these show some good reliability characteristics regarding source Cross-correlation coefficient differences. MUSIC reaches the smallest R-MSE at a low degree of correlation; however, the error gradually increases with increasing; It rises dramatically when the is 0.97-0.99, reaching up to 2.304°. Thus, while MUSIC can make approximate predictions even under conditions of low-source-correlation; however, with an increase in this factor's strength, the system will be more adversely affected. FFT shows that there is a significant difference between low coherence and remains near 2.5°-3.0° in the high-coherence area; However, this medium-error-level does not need to be understood as good-resolution-performance criteria since its correct-resolution-probability has been dropped to zero within the same range of coherences. Among them, CS/OOMP shows the maximum overall error, and its RMSE range is approximately 5.5°-8.3°; Therefore, single-sparsity recovery cannot ensure accurate coherent-source positioning under these conditions.

Together, Figures 9(a)~(b) and Table 4 indicate that LMUSIC has a high consistency in its

correct-resolution probability and is relatively stable in RMSE under various coherence levels. The above results show that in terms of adaptive ability under coherent-source conditions and close-angle resolution reliability compared with FFT, conventional MUSIC and CS/OMP methods.

5 Conclusions

Propose a low-weight high-precision DoA estimation method called L-MUSIC to address the issues of coordination among fast-Fourier transform (FFT), MUSIC and compressed sensing/orthogonal matching pursuit (CS/OMP) techniques in millimetre wave radars with multiple antennas. As MUSIC has been established to provide a good sub-space estimation basis and high-resolution capability; in this paper, by adopting its processing path as the primary research target while reducing the corresponding calculation costs caused by covariance process, eigen-decomposition, etc., for recursive covariance updating method was used to solve this problem. The latter also enhances robustness against a low-SNR, low-signal-noise ratio; weak-array-mismatches condition using diagonal loadings and forward-backward spatial smoothing. An experiment was conducted to provide an in-depth analysis of the eight key indicators for comparing these four methods: spectrum shape and sidelobe suppression; performance at various noise levels (SNR); Computational complexity; Resolution; Stability; Robustness; Low-SNPRace results.; And resolutions under coherent-Source Conditions. According to the above experimental data, L-MUSIC performs better in terms of overall performance than MUSIC under complex scenarios; thus, it is expected to provide good solutions for achieving real-time DOA estimation.

The following three directions of development for future study: Methodological generalisation; System level fusion; Engineering Verification. Although the proposed L-MUSIC has achieved a good balance of resolution, computation time and robustness; at present, its performance is not ideal in some very harsh environment, i.e., high target density, large Array Scale, wide SNR Distributions etc. Secondly, the proposed approach is able to better integrate with the main parts of the Millimeter-Wave Radar Signal-Processing Chain - ranging-Doppler Processing; Target Association and Continuous Sensing - thereby improving the overall Stability and Practicality of DOA Estimation in Dynamic Conditions. Finally, future work needs to strengthen the comparison based on actual measurement results and physical platform; At this time, it will be more effective for L-MUSIC algorithms to perform well in practical deployment environments constrained by low computing power or small memory sizes.

CRediT authorship contribution statement

Tianlong Yang: Review & Editing; Validation; Supervision; Project Administration; Methods and Studies; Investigations; Data Curation; Concepts. Jinqiu Dong: Review and Editing - Writing; Original Draft - Writing; Validation; Software; Funding Acquisition; Data Curation. Zixiang Long: Writing - review and edit; Software: method, methodology; Formal analysis; Data curation; Conceptualisation.

Declaration of competing interest

There are no conflicts of interest or other relationships among the author that might lead to a perceived bias in their publication efforts for this research report.

Acknowledgements

None.

Data availability

You may ask us for it back.

References

[1] Li, H., Wang, H., Cao, J., et al. (2025). A real-time spectrum analysis method using a Zoom-FFT algorithm. Journal of Electronic Measurement and Instrumentation, 39, 32-44.

[2] Zhou, Y., Jiang, W., Zhu, M. H., Chen, X. W., et al. (2024). Equivalent spectral analysis of the mechanical environment for satellites and rockets based on STFT-AOK. Spacecraft Environment Engineering, 41, 11-17.

[3] Kurtoglu, & Rahman, M. (2016). Estimation of the directional arrived signal using virtual antenna arrays with FMCW-radar-simulated data. arXiv, 2025-07513.

[4] Gong, C., Zhang, B. N., & Guo, D. S. (2010). A fast and high-precision joint estimation algorithm of carrier parameters based on FFT. Chinese Journal of Electronics, 38, 766-770.

[5] Zhu, Z., He, L., Zhang, Z., et al. (2023). Frequency-domain analysis method for node pressure in water supply networks based on FFT transformation. Hydropower Energy Science and Technology, 41, 111-114.

[6] Hu, R. J., & Huang, H. Y. (2025). Real-time audio spectrum analysis and dynamic volume control system based on FFT. EIJ, 100803.

[7] Doncui, M. T. C., & Serea, E. (2025). Direct FFT oversampling without zero-padding. Scientific Reports.

[8] Khouilì, O., Haninne, M., Looznàzi, M., & Obiddahlo, W. J. (2025). A high accuracy, lightweight smart solar power prediction based on a shuffled-net and FFT-infusion. International Journal of Electrical Power & Energy Systems, 11124.

[9] Zhu, P., & Wang, R. M. (2025). Low altitude angles measurement based on bidirectional spatial smoothing and MUSIC algorithm for array radar. Naval Electronic Countermeasure, 48(3), 69-74, 97.

[10] Bai, Q. J., Tao, X. J., Wang, A. J., et al. (2024). Sensing array direction-of-arrival method based on Kalman filter and MUSIC algorithm. Hydropower Energy Science and Technology, 42, 217-220.

[11] Li, X., Zhong, T. Z., & Zhong, J. D. (2022). A wide-band signal direction of arrival estimation method using improved MUSIC algorithms. Computer Engineering, 48, 201-

206.

[12] Li, D., Chen, L., Fu, C., Xu, X. J., Gong, Z. R., X., Y. X., & Liu, Z. Y. (2025). Multiple signal classification algorithm-based reflection matrix imaging method for tunnel-array acoustic wave prospecting technology. Journal of Geophysics Research.

[13] Mahgoubi, H., Boussada, A., & Ali, T. (2024). Combination of multiple signal classification algorithm and volume reflectivity models for improving accuracy of estimated vegetation height in synthetic aperture radar tomography. Journal of Applied Remote Sensing, 26(13), 3653-3669.

[14] Takemoto, R., Cha, J., Jeong, I., & Ahn, C. Y. (2024). The effectiveness and features of virtual antennas in multiple signal classification (MUSIC) algorithms. Electronics, 14, 73.

[15] Pan, Y., Zhang, L., Xu, L. Y., & Duan, F. B. (2024). One-bit quantisation observations DOA estimation via noise-enhanced multiple signal classification. Sensors, 24(8), 4719.

[16] Zhong, S. Y., Qiao, M., Liu, Y., Li, et al. (2025). A compressed sensing based reconstruction algorithm of azimuth discontinuity data for IFMCW SAR satellite applications. Journal of the University of Chinese Academy of Sciences, 42, 392-402.

[17] Liu, Y. D., Liang, C. B., Yang, M., et al. (2025). Nuttall window compressed sensing based harmonic and interharmonic detection method. Electronic Measurement Technology, 48, 101-109.

[18] Lin, Z. H., Jia, S. H., Zhang, H. J., Wen, B., Han, M. Y., & Wang, L. N. (2025). A super-resolution phase-reconstruction method based on compressed sensing and deep learning for digital holographic microscopy. Optics and Laser Engineering.

[19] Qin, L., Xu, Y. K., Wang, Y., Xiong, Z. N., & Yi, Y. G. (2025). A sparse Bayesian learning-based network for energy-efficient compressed sensing of ECG signals. Digital Signal Processing, 105608.

[20] Tian, Z. H., Hu, T., Wu, D., Wang, S., Li, T. L., & Zhang, M. (2025). A frequency-orthogonal attention-joined optimisation network for image compression sensing. Expert Systems, 129866-130124.

[21] Schmidt, R. O. (1986). Multiple emitter location and signal parameter estimation. IEEE Transactions on Antennas and Propagation, 34(3), 276-280.

[22] Roy, R., & Kailath, T. (1989). ESPRIT-estimation of signal parameters via rotational invariant techniques. IEEE Transactions on Acoustics, Speech, and Signal Processing, 37(7), 984-995.

[23] Stoica, P., & Nehorai, A. (1989). MUSIC, maximum likelihood, and Cramer-Rao bounds. IEEE Transactions on Acoustics, Speech, and Signal Processing, 37(5), 720-741.

[24] Van Veen, B. D., & Buckley, K. M. (1988). Beamforming: A general method for spatial filtering. IEEE ASSP Magazine, 5(2), 4-24.

[25] Shan, S. J., Wax, M., & Kailath, T. (1985). Spatial smoothing and coherent signals'

direction of arrival estimation. IEEE Transactions on Acoustics, Speech, and Signal Processing.

[26] Pillai, S. U., & Kwon, B. H. (1989). Forward/backward spatial smoothing techniques for coherent signal recognition. IEEE Transactions on Acoustics, Speech, and Signal Processing, 37(1), 8-15.

[27] Friedlander, B., & Weiss, A. J. (1992). Direction finding via spatial smoothing on interpolated arrays. IEEE Transactions on Aerospace and Electronic Systems, 28(2), 574-587.

[28] Van der Veen, A. J., Deprettere, E. F., & Swindlehurst, A. B. (1993). Subspace-based signal analysis through singular value decomposition. Proceedings of the IEEE, 81(9), 1277-1308.

[29] Ottersten, B., Viberg, M., & Kailath, T. (1991). Detection and estimation in sensor arrays based on weighted subspace fitting. IEEE Transactions on Signal Processing, 39(11), 2436-2449.

[30] Wu, D., & Kirlin, R. B. (1991). Improvements to spatial smoothing techniques for coherent signals in DOA estimation. IEEE Transactions on Signal Processing, 39(5), 1208-1210.

[31] Malioutov, D., Çetin, M., & Willsky, A. S. (2005). A sparse signal reconstruction-based perspective for source localisation using sensor arrays. IEEE Transactions on Signal Processing.

[32] Blanco, & Najar. (2012). Sparse covariance estimation based on direction of arrival. EURASIP Journal on Advances in Signal Processing, 2012(11), 111.

[33] Yin, J., & Chen, T. (2011). Direction-of-arrival estimation based on sparse representation of array covariance vectors. IEEE Transactions on Signal Processing, 59(9), 4489-4493.

[34] Li, J., Stoica, P., & Wang, Z. (2003). On robust Capon beamforming and diagonal loading. IEEE Transactions on Signal Processing, 51(7), 1702-1715.

[35] Chen, J., Wu, Y., Cao, H., & Wang, H. (2011). Fast algorithm for DOA estimation based on partial covariance matrix and without eigendecomposition. Journal of Signal and Information Processing, 2(4), 266-269.

[36] Cai, S., Wang, G., Zhang, J., Wong, K.-K., & Zhu, H. (2017). Sparse covariance fitting-based efficient direction-of-arrival (DOA) estimation in the presence of model misalignment. Signal Processing, 137, 264-273.

[37] Sun, X.-Y., Zhou, J.-J., & Chen, H.-W. (2016). Low-complexity direction-of-arrival (DOA) estimation for coherent non-circular sources. Multidimensional Systems and Signal Processing, 27(1), 159-177.

[38] Wen, J., Liao, B., & Guo, C. (2017). Spatial smoothing-based methods for direction-of-arrival estimation of coherent signals in non-uniform noise. Digital Signal Processing, 67, 116-122.

[39] Yang, M., Zhang, Y., Sun, Y., & Zhang, X. (2023). Enhanced spatial smoothing technique for coherent direction-of-arrival estimation using moving coprime array. Sensors, 23(19), 8048.

[40] Wang, W., Zheng, T., Yao, B., Wang, W., & Xiu, X. (2023). Low complexity direction-of-arrival estimation algorithm of non-circular signals by subspace rotation technique. International Journal of Antennas and Propagation, 2023, 8622428.